NRL Memorandum Report 5154

Dynamic Design Analysis of a Foundation Undergoing Unequal Support Shock Motion

GEORGE J. O'HARA AND PATRICK F. CUNNIFF

Structural Integrity Branch
Marine Technology Division

September 22, 1983

NAVAL RESEARCH LABORATORY
Washington, D.C.

SECURITY CLASSIFICATION OF THIS PAGE (When Data Entered)

REPORT DOCUMENTATION PAGE		READ INSTRUCTIONS BEFORE COMPLETING FORM
1. REPORT NUMBER NRL Memorandum Report 5154	2. GOVT ACCESSION NO. AD-A133071	3. RECIPIENT'S CATALOG NUMBER
4. TITLE (and Subtitle) DYNAMIC DESIGN ANALYSIS OF A FOUNDATION UNDERGOING UNEQUAL SUPPORT SHOCK MOTION		5. TYPE OF REPORT & PERIOD COVERED Interim report on a continuing NRL problem. 6. PERFORMING ORG. REPORT NUMBER
7. AUTHOR(s) George J. O'Hara and Patrick F. Cunniff		8. CONTRACT OR GRANT NUMBER(s)
9. PERFORMING ORGANIZATION NAME AND ADDRESS Naval Research Laboratory Washington, DC 20375		10. PROGRAM ELEMENT, PROJECT, TASK AREA & WORK UNIT NUMBERS SF 43-400-001 DTNSRDC 23102 58-1345-00
11. CONTROLLING OFFICE NAME AND ADDRESS		12. REPORT DATE September 22, 1983 13. NUMBER OF PAGES 30
14. MONITORING AGENCY NAME & ADDRESS(if different from Controlling Office)		15. SECURITY CLASS. (of this report) Unclassified 15a. DECLASSIFICATION/DOWNGRADING SCHEDULE

16. DISTRIBUTION STATEMENT (of this Report)

Approved for public release; distribution unlimited.

17. DISTRIBUTION STATEMENT (of the abstract entered in Block 20, if different from Report)

18. SUPPLEMENTARY NOTES

19. KEY WORDS (Continue on reverse side if necessary and identify by block number)

Foundation design
Shipboard shock
Dynamic design

20. ABSTRACT (Continue on reverse side if necessary and identify by block number)

A design analysis method developed earlier for small shipboard foundations is extended to those cases where the foundation supports experience unequal levels of shock excitation. The method utilizes an energy criterion such that the foundation may remain elastic or may experience elastic-plastic behavior in such a way as to insure against large deflections or unwanted collapse. Predicted load carrying capacity levels are developed for a sample foundation undergoing unequal support motion. In addition, results are compared with these obtained

(Continued)

DD FORM 1 JAN 73 1473 EDITION OF 1 NOV 65 IS OBSOLETE
S/N 0102-014-6601

SECURITY CLASSIFICATION OF THIS PAGE (When Data Entered)

20. ABSTRACT (Continued)

earlier for equal levels of shock excitation of the foundation supports. The results are worked up in detail, both theoretically and by numerical examples to show the ease of application and efficiency of the method.

CONTENTS

DYNAMIC DESIGN ANALYSIS OF A FOUNDATION UNDERGOING UNEQUAL SUPPORT SHOCK MOTION

INTRODUCTION

A design procedure for small shipboard foundations undergoing mechanical shock excitation has been the subject of earlier reports [1,2]. The design method is applicable to equipment-foundation combinations that may be modeled as single-degree-of-freedom (SDOF) systems. Since the static and dynamic stress and deflection patterns are the same for such systems. the actual energy stored in the foundation as the system undergoes shock excitation may be compared with the total energy storage capacity of the foundation. This approach provides the basis of an efficient design method of SDOF systems that allows the foundation material either to remain elastic throughout the shock excitation or to experience some degree of plastic action.

The purpose of this report is to extend the application of the energy design method to those cases where the foundation supports experience unequal levels of shock excitation and to compare the results with those obtained earlier for equal levels of shock excitation of the foundation supports. A review of both the elastic and elastic-plastic design methods are also included for completeness of this report.

BACKGROUND

A. Equipment Foundation System

Consider the SDOF system attached to a moveable base as shown in Fig. 1. Let $\bar{w}$ be the weight of the equipment and an assigned portion of the foundation weight. The equipment foundation system is designed to withstand the lesser of a 250-g equivalent static acceleration or a design shock spectrum velocity level, V_d, equal to 8 ft/sec. Note that $V_d = 2\pi fX$, where f = natural frequency of the system and X = relative displacement between the mass and the base.

For the spectrum velocity shock input let U_r be the maximum kinetic energy of the SDOF system that the foundation must absorb, while U_f is the energy storage capacity of the system. The survival criteria for the equipment foundation combination is

$$U_r \leqslant U_f. \tag{1}$$

That is, the maximum energy stored in the foundation must be less than or equal to the energy storage capacity of the foundation in order for the structure to survive the shock excitation. Note that it is assumed that no energy is stored in the equipment.

Now consider the two propped cantilever beams shown in Fig. 2 that form the foundation for a rigidly attached equipment. Each beam is a 10 WF 25 structural member and it is assumed that they share equally the load in vertical shock. The material is steel with a tensile and compressive yield point of 50 ksi and a shear yield of 25 ksi. Young's modulus $E = 30 \times 10^6$ psi and the shear modulus $G = 12 \times 10^6$ psi. Figure 3 shows the critical dimensions of the cross-section of one of the beams.

Manuscript approved May 19, 1983

B. Method of Analysis

Figure 4 is a model of one of the propped beams in which loads w are placed at the points of attachment of the equipment (whose total weight equals 4 w) to the beam. Note that in this report the SDOF system contains two discrete masses. Replace each equipment load w by a force of magnitude P as shown in Fig. 5. Let P be the maximum allowable force that the beam can withstand for either elastic response or elastic-plastic response to occur under shock excitation.

The energy storage capacity of the beam consists of the bending energy U_b and the shear energy U_s, which are defined as follows:

$$U_b = \int_0^L \frac{M^2 dx}{2EI} \tag{2}$$

$$U_s = \int_0^L \frac{\alpha S^2 dx}{2AG} \tag{3}$$

where M = bending moment, S = shear, I = moment of inertia, A = cross-sectional area, α = ratio of A to the web area, and L = length of the beam. Note that α is arbitrarily set equal to unity in the elastic-plastic design method in order to provide a conservative design. It is also noted that the earlier results [1, 2] used beam reactions that were based on bending effects only. This assumption is now substantiated by the results of Appendix A which examines the energy calculations when the shear effects are included along with bending effects for determining the beam reactions and deflections.

C. Equal Support Motion Results

A summary of previous results [1, 2] for equal support shock excitation levels is shown in Table 1. The data list the allowable weights that each propped beam may carry for the elastic failure criteria and for the elastic-plastic analysis using the combined stress resultant failure criteria that is described in Ref. 2. The design loads of 242.0 lb for the elastic design and 828.8 lb for the elastic-plastic design will be used as the basis of comparison between equal and unequal foundation shock excitation.

Table I — Summary
of Allowable Weights (lb)
Carried by One Beam

Failure Criteria	Design Approach	
	250-g	Energy
Absolute Elastic	157.4	242.0
Elastic-Plastic	376.4	828.8

SHOCK EXCITATION MODEL

Suppose one of the foundation supports of the propped beam undergoes a shock excitation level that is different from that experienced by the other foundation support. It is assumed that the inertial forces and spectral velocities are distributed linearly along the length of the two-mass model of the beam as shown in Fig. 6, where Fig. 6(a) is the case for maximum motion occurring at the pinned end, while Fig. 6(b) is for the maximum motion occurring at the clamped end. Note that β is a proportionality factor such that

$$0.5 \leqslant \beta \leqslant 1. \tag{4}$$

When $\beta = 0.5$, one end of the beam remains stationary. Of course, the case of equal support motion occurs when $\beta = 1$ which was treated earlier [1, 2].

Figure 7 represents the shock levels for the assumed distribution shown in Fig. 6, where the shock levels are expressed in terms of the equivalent static acceleration levels N_i and the design shock spectrum velocity levels V_i where i refers to the station location. Note that the maximum shock levels occur at the end supports of the beam. The shock magnitudes at the beam supports may be expressed in terms of the shock magnitudes at station 1 or station 2 by means of Fig. 6. For example, in the case of maximum motion of the pinned end shown in Fig. 7(a),

$$N_0 = (2 - \beta) N_1 \tag{5a}$$

$$N_3 = (2\beta - 1) N_1 \tag{5b}$$

$$V_0 = (2 - \beta) V_1 \tag{5c}$$

$$V_3 = (2\beta - 1) V_1. \tag{5d}$$

For maximum motion at the clamped end of the beam as depicted by Figs. 6(b) and 7(b),

$$N_0 = (2\beta - 1) N_2 \tag{6a}$$

$$N_3 = (2 - \beta) N_2 \tag{6b}$$

$$V_0 = (2\beta - 1) V_2 \tag{6c}$$

$$V_3 = (2 - \beta) V_2. \tag{6d}$$

ELASTIC ANALYSIS

A. Elastic Failure Criteria

The following describes the application of the elastic design method for the case in which the maximum shock motion occurs at the pinned end of the propped beam as shown in Fig. 7(a). For this shock loading configuration apply the maximum allowable forces P and βP on the beam as shown in Fig. 8(a). The corresponding shear and bending moment diagrams are shown in Figs. 8(b) and 8(c). For an elastic design, the first step is to examine again the following elastic failure criteria utilizing Fig. 3:

Case a — Flange-web elastic failure in combined stress (see point a in Fig. 3);

Case b — Shear failure at the center of the web (see point b in Fig. 3);

Case c — Bending stress at the outer fiber (see point c in Fig. 3).

These three cases are now presented in greater detail. Sample calculations are also provided in Appendix B for further clarification.

Case a: The maximum shearing stress is governed by the following relationship:

$$\tau_{max} = \sqrt{\left[\frac{\sigma_b}{2}\right]^2 + \tau_{xy}^2} \tag{7}$$

where τ_{max} = allowable maximum shear stress = 25,000 psi

$$\sigma_b = \text{bending stress} = \frac{Mc}{I} \tag{8}$$

$$\tau_{xy} = \text{shear stress} = \frac{VQ}{Ib}. \tag{9}$$

For the shear and bending moment diagrams in Fig. 8, the critical cross-section of the beam occurs at the clamped end where both the shear and bending moment values are a maximum.

Case b: The maximum shear occurs at the clamped end. Here, $V = \frac{P}{27}(13 + 23\beta)$. Substituting the maximum shear stress value of 25,000 psi into Eq. (9) along with the beam properties Q, I, and b, the magnitude of P is calculated for a given value of β.

Case c: Again, the critical beam cross-section occurs at the clamped end where $M = \frac{10P}{3}(4 + 5\beta)$. Setting the maximum allowable bending stress equal to 50,000 psi into Eq. (8), the allowable load P is calculated for any given value of β.

It is interesting to note that for $\beta = 1$, $P = 35,310$ lb which agrees with earlier results [1]. For maximum motion of the pinned end and for $\beta = 0.5$, $P = 50,215$ lb which represents the upper limit of P for all values of β given by Eq. (4).

B. Equivalent Static Acceleration Design Method

Having established the allowable value of P for a given β, the load carrying capacity of the propped beam is found for the equivalent static accelertion design criteria as follows:

$$P + \beta P = \bar{w}\, N \tag{10}$$

where $\bar{w}$ = total weight of the SDOF model for one beam

$$= 2w + 2w_f \text{ (refer to Fig. 4)} \tag{11}$$

w_f = portion of the beam weight assumed at each point mass = 62.5 lb

Due to the uneven distribution of the shock excitation as shown in Fig. 7(a) for maximum motion of the pinned end, rewrite Eq. (10) as follows:

$$P(1 + \beta) = \frac{\bar{w}}{2} N_1 + \frac{\bar{w}}{2} N_2 \tag{12}$$

where $N_2 = \beta\, N_1$ as shown in Fig. 6(a). Now

$$P = \frac{\bar{w}}{2} N_1 \tag{13}$$

or the load carrying capacity of one beam equals the following:

$$2w = \frac{2P}{N_1} - 2w_f. \tag{14}$$

This equation may be expressed in terms of the maximum shock level occurring at the pinned end by means of Eq. (5a), i.e.,

$$2w = \frac{(2 - \beta)\,(2P)}{N_0} - 2w_f. \tag{15}$$

For example, if $N_0 = 250$ g's and $\beta = 0.5$, the load carrying capacity of the beam equals

$$2w = \frac{(2 - 0.5)\,(2)\,(50,215)}{250} - 125 = 477.6 \text{ lb.}$$

C. Energy Design Method

In order to analyze the beam foundation for the design shock spectrum velocity levels shown in Fig. 7(a), the energy storage capacity of the beam is calculated using Eqs. (2) and (3), or directly from the shear and moment diagrams, i.e., by taking the moment of the shear and moment diagrams, properly scaled, about their respective base lines. Details of the latter proceedure are given in Appendix B.

For example, using the data in Fig. 8 and $\beta = 0.5$ and $P = 50,215$ lb, the total energy storage capacity $U_t = 5423$ lb-in. The actual stored energy is obtained from the maximum kinetic energy of the SDOF system, i.e.,

$$U_r = \frac{1}{2}\left(\frac{\bar{w}}{g}\right) V^2 = \frac{1}{2}\left[\frac{\bar{w}}{2g} V_1^2 + \frac{\bar{w}}{2g} V_2^2\right] \tag{16}$$

where $V_2 = \beta V_1$ for maximum motion of the pinned end of the beam. For the survival criteria, let $U_r = U_t$. Substituting these relationships along with Eq. (11) into Eq. (16) and rearranging terms, the following expression results:

$$2w = \frac{4g\ U_t}{(1+\beta^2)\ V_1^2} - 125. \tag{17}$$

Substituting Eq. (5c) into Eq. (17) for the case of maximum motion of the pinned end leads to the following expression for the load carrying capacity of the beam:

$$2w = \frac{4g(2-\beta)^2\ U_t}{(1+\beta^2)\ V_0^2} - 125. \tag{18}$$

If $\beta = 0.5$, $U_t = 5,423$ lb-in., and if $V_0 = 96$ in./sec, the load carrying capacity equals 1,512 lb.

Note that the foregoing results are applicable to the case in which maximum motion occurred at the pinned end of the beam. Similar results could also be obtained for maximum motion of the clamped end so that the maximum force P would now be acting at station 1 and the force βP would be acting at station 2.

ELASTIC-PLASTIC ANALYSIS

A. Limit Analysis

The first step in the elastic-plastic energy design method is to locate the plastic hinges for the structure using limit analysis. Figure 9 shows the location of the hinges for maximim shock motion of the pinned end, while Fig. 10 provides the shear and bending moment diagrams for the case where $\beta = 0.5$. Next, consider the interaction relationship between the shear force S and bending M as reported in Ref. 2:

$$\left(\frac{M}{M_p}\right)^2 = 1 - \left(\frac{S}{S_p}\right)^2 \tag{19}$$

where M_p = limiting value of the bending moment in the absence of shear forces
S_p = limiting value of the shear force in the absence of bending moments.

This relationship must be satisfied at each of the plastic hinge locations which has the effect of adjusting the final shear and moment values throughout the beam. By examining the free-body diagram of the beam to the left of the hinge at station 1 in Fig. 11, $S = R_L$ and $M = 30\ R_L$. Substituting into Eq. (19) along with $S_p = 184,000$ lb and $M_p = 1,483,000$ in.-lb for the given beam properties, the following maximum reaction at the pinned end is found:

$$R_L = \frac{M_p\ S_p}{[900\ S_p^2 + M_p^2]^{1/2}} = 47,740 \text{ lb.}$$

At the clamped end of the beam the moment $M = M_R = (30\ \beta P + 60\ P - 90\ R_L)$ and the shear $S = (P + \beta P - R_L)$. Substituting into Eq. (19) yields $P = 75,750$ lb. This is the magnitude of the force P applied to the beam in Fig. 9 such that Eq. (19) is satisfied at stations 1 and 3 simultaneously.

It should be noted that the location of the plastic hinges may change from that predicted by simple limit analysis because of the interaction effects. This is so since limit analysis utilizes bending effects only while the interaction equation includes both bending and shearing effects. For example, for the maximum shock motion occurring at the clamped end of the beam, the plastic hinges are located at stations 1 and 3 for β greater than 0.5 and less than or equal to unity by limit analysis. Upon further investigation, however, the interection effects of shear and bending as expressed by Eq. (19) locate the hinges at stations 2 and 3 for $\beta < 0.6265$. For $\beta > 0.6265$, the hinge at station 2 shifts to station 1 while the hinge at station 3 remains fixed for all values of β. The details for the special situation when $\beta = 0.6265$ in which there are three hinges present simultaneously are found in Appendix C.

B. Equivalent Static Acceleration Design Method

Equation (15) is also applicable for obtaining the load carrying capacity of the beam by the elastic-plastic design method for maximum motion occurring at the pinned end of the beam. For example, in the above case of $\beta = 0.5$, substituting $P = 75,750$ lb and $N_0 = 250$ g's into Eq. (15) yields a value $2w = 783.8$ lb.

C. Energy Design Method

The procedure for calculating the load carrying capacity of the beam for the elastic-plastic energy design approach is similar to that used for the elastic energy design method. For example, consider Fig. 10 which shows the shear and bending moment diagrams for $\beta = 0.5$. Note that $P = 75,750$ lb as explained earlier. The total energy storage capacity for this loading equals 9,644 lb-in. Using Eq. (18) for maximum motion of the pinned end of the beam, the load carrying capacity equals 2,786 lb. Details for applying the elastic-plastic method for the case where maximum motion occurs at the clamped end of the beam are found in Appendix B.

EQUAL VERSUS UNEQUAL SHOCK EXCITATION

It is interesting to examine an equipment foundation system that has already been designed for equal shock excitation, that is, a system capable of withstanding the lesser of a 250-g equivalent static acceleration or a design shock spectrum velocity level of 8 ft/sec. The results of this analysis have already been summarized in Table I. For example, according to the elastic failure criteria one of the propped beams can carry a load of 242.0 lb based on the energy design method. Suppose this same equipment foundation system is now subjected to unequal shock excitation at the foundation supports. The following question arises: what are the maximum shock levels at the foundation support points that this system can withstand for a given β?

Consider the case in which the maximum excitation occurs at the pinned end of the beam. The maximum allowable equivalent static acceleration level N_0 is obtained by rearranging Eq. (13) so that

$$N_1 = \frac{2P}{\bar{w}}$$

or by introducing Eq. (5a),

$$N_0 = \frac{(2-\beta)\,(2P)}{\bar{w}}. \tag{20}$$

The static acceleration level at the clamped end of the beam is found by using Eq. (5b), i.e.,

$$N_3 = \frac{(2\beta-1)\,(2P)}{\bar{w}}. \tag{21}$$

For the beam carrying 242.0 lb,

$$\bar{w} = 242.0 + 125.0 = 367.0 \text{ lb}.$$

For the case where $\beta = 0.5$, $P = 50,215$ lb as mentioned earlier. Therefore, $N_0 = 410.5$ g's and $N_3 = 0$ by means of Eqs. (20) and (21), respectively. That is, the equipment foundation system that was originally designed for equal shock levels at each foundation support may withstand up to 410.5 g's at the pinned end of the beam while the clamped end experiences a zero g-level.

The maximum shock levels in terms of the design shock spectrum velocity may be obtained in a similar fashion by rearranging Eq. (17) as follows:

$$V_1 = \sqrt{\frac{4g\ U_t}{(1+\beta^2)\,\bar{w}}}.$$

Substituting Eqs. (5c) and (5d) into this equation, the spectrum velocity levels at the end supports are found as follows:

$$V_0 = (2-\beta)\sqrt{\frac{4g\ U_t}{(1+\beta^2)\,\bar{w}}} \tag{22}$$

$$V_3 = (2\beta-1)\sqrt{\frac{4g\ U_t}{(1+\beta^2)\,\bar{w}}}. \tag{23}$$

Once again, consider the case where $\bar{w} = 367.0$ lb, $\beta = 0.5$, and $U_t = 5,423$ lb-in for elastic behavior of the beam. Equations (22) and (23) yield $V_0 = 16.90$ ft/sec and $V_3 = 0$, respectively. Thus, a foundation system designed to withstand a design shock spectrum level of 8 ft/sec at each support can withstand a level of 16.9 ft/sec at the pinned end of the beam when the clamped end remains stationary.

RESULTS

The results for the load carrying capacity of one of the beams that form the foundation are shown in Fig. 12. The abscissa is divided into two regions identified as the clamped/pinned ratio which equals $(2\beta - 1)/(2 - \beta)$ from Fig. 6(a), while the pinned/clamped ratio has a similar relationship as seen in Fig. 6(b). The results in Fig. 12 are for maximum end support shock levels of 250 g's and 8 ft/sec. Both elastic and elastic-plastic design results are included in the figure. In all cases it is seen that the load carrying capacity increases significantly as β approaches 0.5, that is, as the clamped/pinned ratio and the pinned/clamped ratio each approach zero. For example, when both foundations move alike, the load carrying capacity based upon the elastic energy design is 242.0 lb. This energy design level increases to 1,512 lb for the case when $\beta = 0.5$ for the pinned end undergoing shock excitation while the other end of the beam remains fixed. From the shape of these curves in Fig. 12, it is clear that the most severe design criteria occur when both supports move an equal amount, i.e., $\beta = 1$.

The elastic energy design curve for predicting the load carrying capacity and the corresponding elastic-plastic equivalent static acceleration design curve cross each other at two locations as shown in Fig. 12. For example, in the clamped/pinned region, the crossover occurs at β equal to approximately 0.85. For $\beta < 0.85$, higher allowable loads are predicted by the elastic energy design method over the elastic-plastic equivalent static acceleration design method. Similar results hold true for the pinned/clamped region for $\beta < 0.6$, although the effect is much less pronounced.

Another interesting observation of the curves in Fig. 12 occurs in the reversal of the load carrying capacity levels. The larger elastic capacity levels occur for maximum motion at the pinned end of the beam, while the larger elastic-plastic capacity levels occur for maximum motion at the clamped end of the beam. These phenomena are due primarily to the shape of the bending moment diagrams as shown in Fig. 13. These curves, drawn for $\beta = 0.5$, are used with Eq. (2) to obtain the bending energy storage capacity. It is noted that the U_b obtained from Fig. 13(a) is larger for the pinned end motion of the beam. Hence, a larger carrying capacity is obtained for the elastic design approach. Just the opposite occurs when U_b is calculated by means of Fig. 13(b), so that a larger carrying capacity is obtained for the clamped end motion in the case of the elastic-plastic design method.

Figure 14 is a summary of the results for the case where a beam, designed for equal support motion, is examined for the maximum allowable shock levels when this beam undergoes unequal foundation motion. Both elastic and elastic-plastic design level results are included in Fig. 14. Note that the g-levels in the left portion of the figure correspond to the equivalent static acceleration levels at the pinned end, namely N_0, while those levels in the right portion of the figure correspond to the clamped end levels N_3. Likewise, Fig. 15 shows the results for the same beam examined in terms of the design shock spectrum velocity limits.

Similar results are shown in Figs. 16 and 17 for the case of the beam designed for equal foundation motion by the elastic-plastic energy method. The load carrying capacity of the beam for this case equals 828.8 lb as shown in Table 1.

SUMMARY

The extension of the elastic and elastic-plastic design methods developed earlier to those cases where unequal shock levels occur at the support points provide some interesting results. While the assumption is made that the unequal shock level inputs in terms of the inertial forces and spectral velocities are distributed linearly between the support points of the propped beams has not been validated, the results do provide an indication of the change in strength of the foundation beams. Thus, for $\beta = 0.5$ for all cases studied, the load carrying capacity increases significantly when compared with equal shock level inputs for $\beta = 1$. Likewise, the analysis showed that foundations already designed for equal shock loading at the support points can withstand correspondingly larger shock level inputs at the support point undergoing maximum motion.

REFERENCES

1. O'Hara, G.J. and Cunniff, P.F., "Efficient Elastic Design of Small Foundations," NRL Memorandum Report 4886, September 1982.

2. O'Hara, G.J. and Cunniff, P.F., "Efficient Elastic-Plastic Design of Small Foundations," NRL Memorandum Report 4918 September 1982.

3. Blake, R.E. and Swick, E.S., "Dynamics of Linear Elastic Structures," NRL Report 4420, October 1954.

4. Timoshenko, S. and MacCullough, G.H., "Elements of Strength of Materials," D. Van Nostrand Co., 3rd Edition, 1949, p. 195.

Appendix A
EFFECTS OF SHEAR ON ENERGY CALCULATIONS

The calculation of the elastic energy storage capacity has been made using standard structural analysis techniques in which support reactions and beam deflections include bending effects only. However, it is known that for small values of the L/r ratio, deflections due to shear do alter the beam reactions somewhat significantly. The subsequent error in the energy calculations when shear effects are included in the analysis is the subject of this appendix.

The energy stored in the propped cantilever beam shown in Fig. A-1 is given [3] by the expression

$$U = \frac{1}{2} P^2 \Delta_{11} + \frac{1}{2} P^2 \Delta_{22} + P^2 \Delta_{12} \tag{A.1}$$

where Δ_{ij} is the influence coefficient representing the deflection at point i due to the load at point j. The deflection due to bending and shear effects are included in the following analysis.

Figure A-2 shows the free-body diagram of the beam with a single load P acting at station 1. The reactions are

$$R_L = \frac{14\, P(\phi^2 + \frac{27}{7}\epsilon)}{27(\phi^2 + 3\epsilon)} \tag{A.2}$$

$$R_R = \frac{13P\ (\phi^2 + \frac{27}{13}\epsilon)}{27\ (\phi^2 + 3\epsilon)} \tag{A.3}$$

$$M_R = \frac{4\, PL\ \phi^2}{27(\phi^2 + 3\epsilon)} \tag{A.4}$$

where $\phi = \frac{L}{r}$, $r^2 = \frac{I}{A}$, $\epsilon = \gamma\alpha$, $\gamma = \frac{E}{G}$, and α = ratio of A to the web area. It is interesting to note that as ϕ^2 approaches zero, the reactions reduce to the values of the reactions for a simply supported beam with shear effects only, and as ϕ^2 approaches infinity, the reactions reduce to the reactions for the propped beam when bending effects are present only. For example, in the case of the right reaction,

$$\lim_{\phi^2 \to 0} R_R = \frac{P}{3}$$

$$\lim_{\phi^2 \to \infty} R_R = \frac{13P}{27}.$$

Next consider Fig. A-3 which shows the XY coordinate system for which the curvature equation of the beam [4] is as follows:

$$\frac{d^2y}{dx^2} = -\frac{M}{EI} + \frac{\alpha}{AG}\left[\frac{dV}{dx}\right] \tag{A.5}$$

where $M = R_R\, x - M_R$. Now integrate Eq. (A.5) for the beam in Fig. A-2 noting that $V = R_R$ for $x < 2L/3$.

$$\frac{dy}{dx} = -\frac{R_R x^2}{2\,EI} + \frac{M_R\,x}{EI} + \frac{\alpha\,R_R}{AG} + C_1. \tag{A.6}$$

The constant of integration C_1 is obtained using the boundary condition that at $x = 0$, $\frac{dy}{dx} = \frac{\alpha R_R}{AG}$. Thus, $C_1 = 0$. Integrating Eq. (A.6) and noting that at $x = 0$, $y = 0$, leads to the following for $x = 2L/3$:

$$y = -\frac{4\,M_R L^3}{81\,EI}\left[1 - \frac{9\,M_R}{2L\,R_R} - \frac{27\,\alpha\,EI}{2\,AGL^2}\right]. \tag{A.7}$$

Substituting Eqs. (A.3) and (A.4) into Eq. (A.7) and letting $P = 1$ yields the influence coefficient

$$\Delta_{11} = \frac{2\,L^3\,(10\,\phi^4 + 297\,\epsilon\,\phi^2 + 729\,\epsilon^2)}{2187\,EI\,\phi^2\,(\phi^2 + 3\epsilon)}. \tag{A.8}$$

Note that

$$\lim_{\phi^2 \to 0} \Delta_{11} = \frac{2\alpha L}{9\,AG} = \text{shear deflection of a simply supported}$$

beam subjected to a unit load at station 1. Also,

$$\lim_{\phi^2 \to \infty} \Delta_{11} = \frac{20\,L^3}{2187\,EI} = \text{bending deflection of the propped}$$

beam subjected to a unit load at station 1.

Similar results may be obtained for the remaining influence coefficients that are summarized as follows:

$$\Delta_{21} = \Delta_{12} = \frac{L^3\,(23\,\phi^4 + 675\,\epsilon\,\phi^2 + 1458\,\epsilon^2)}{4374\,EI\,\phi^2(\phi^2 + 3\epsilon)} \tag{A.9}$$

$$\Delta_{22} = \frac{L^3(22\phi^4 + 1188\,\epsilon\,\phi^2 + 2916\,\epsilon^2)}{4374\,EI\,\phi^2\,(\phi^2 + 3\epsilon)}. \tag{A.10}$$

These values for the influence coefficients are now substituted into Eq. (A.1) to give the following:

$$U = \frac{P^2 L^3\,(6\phi^4 + 207\,\epsilon\phi^2 + 486\,\epsilon^2)}{486\,EI\,\phi^2(\phi^2 + 3\epsilon)}. \tag{A.11}$$

Using the properties of the 10 WF 25 beam shown in Fig. 3 yields $\phi = 21.14$ and $\epsilon = 7.92$. For these values

$$U = \frac{P^2}{285,690}. \tag{A.13}$$

This energy level compares with $U = P^2/(284,900)$ as reported in Ref. [1] when the contribution of shear to the beam reactions and beam deflections were omitted. Figure A-4 summarizes the percent error between the two methods for calculating U as a function of ϕ. The error is less than two percent for L/r ratios greater than 10. Consequently, this error is insignificant for most beams used in practice. Note that $\phi = 21.14$ for the propped beam examined in this report, so that the error is less than 0.5% for the energy calculations made herein and in earlier reports [1,2].

Appendix B
SAMPLE COMPUTATIONS

A. Elastic Failure Criteria

As an example of the elastic failure criteria consider the propped beam in Fig. 8 where $\beta = 0.5$. The maximum shear and bending moment occur at the fixed end where

$$V = \frac{P}{27}(13 + 23\beta) = 0.907407\ P$$

$$M = \frac{10P}{9}(12 + 15\beta) = 21.667\ P.$$

Case a

$$\sigma_b = \frac{Mc}{I} = \frac{(21.667\ P)\ (4.603)}{133.2} = 0.748748\ P$$

$$\tau_{xy} = \frac{VQ}{Ib} = \frac{(0.907407\ P)\ (12.14)}{(133.2)\ (0.252)} = 0.328183\ P.$$

Substitute into Eq. (7).

$$(25,000)^2 = \left[\frac{0.748748\ P}{2}\right]^2 + (0.328183\ P)^2$$

$$P = 50,215 \text{ lb.}$$

Case b

For the shear failure at the center of the beam,

$$\tau = 25,000 = \frac{(0.907407\ P)\ (14.81)}{(133.2)\ (0.252)}$$

$$P = 62,444 \text{ lb}$$

Case c

For bending failure,

$$\sigma = 50,000 = \frac{(21.667\ P)\ (5.04)}{133.2}$$

$$P = 60,988 \text{ lb.}$$

Case a provides the smallest value so that $P = 50,215$ lb is the design load.

Figure B-1 shows the shear and moment diagrams for $\beta = 0.5$ when the maximum motion occurs at the pinned end. The energy due to shear is calculated directly from the shear diagram as follows:

$$U_s = \frac{\alpha}{AG}\left[\frac{30}{2}(0.592593)^2 + \frac{30}{2}(0.407407\ P)^2 + \frac{30}{2}(0.907407\ P)^2\right]$$

$$= \frac{1}{AG}\left[\frac{A}{A_w}\right](20.108)P^2 = \frac{1}{12 \times 10^6 \times 2.32}(20.108)\ (50,215)^2$$

$$= 1821.2 \text{ lb-in.}$$

For the bending energy,

$$U_b = \frac{1}{EI}\left\{\frac{1}{2}\left[\frac{30}{3}\right](17.778\ P)^2 + \frac{1}{2}(17.778 - 5.556)\ P(30)\left[5.556\ P + \frac{12.222\ P}{3}\right]\right.$$

$$\left. + \frac{30}{2}(5.556\ P)^2 + \frac{1}{2}\left[\frac{6.122}{3}\right](5.556\ P)^2 + \frac{1}{2}\left[\frac{23.878}{3}\right](21.667\ P)^2\right\}$$

$$U_b = \frac{5708.5\ P^2}{EI} = \frac{5708.5\ (50,215)^2}{30 \times 10^6 \times 133.2} = 3602.2 \text{ lb-in}$$

$$U_t = U_s + U_b = 5423.4 \text{ lb-in.}$$

B. Elastic-Plastic Analysis

The sample computations for the elastic-plastic design method are for the case where maximum motion occurs at the clamped end of the beam and $\beta = 0.5$. Figure B-2(a) shows the free body diagram of the beam. Surprisingly, the theory of limit analysis predicts plastic hinges occurring simultaneously at stations 1, 2, and 3. However, the interaction equation for bending and shear should be satisfied. In order to locate these positions, consider Fig. B-2(b) that shows the free body diagram of the beam to the right of station 2. Now

$$M_2 = 30\ R_R - M_R. \tag{B.1}$$

Assuming there are hinges at stations 2 and 3, $M_2 = M_R$ so that

$$M_R = 15\ R_R. \tag{B.2}$$

From Fig. B-2(a),

$$90\ R_R = M_R + 30\ (0.5\ P) + 60\ P. \tag{B.3}$$

Substituting for R_R from Eq. (B.2), Eq. (B.3) reduces to $M_R = 15\ P$ and therefore, $R_R = P$.

Apply Eq. (19) at either station 2 or station 3 as follows:

$$\left(\frac{M}{M_p}\right)^2 + \left(\frac{S}{S_p}\right)^2 = 1$$

so that

$$\left(\frac{15\ P}{M_p}\right)^2 + \left(\frac{P}{S_p}\right)^2 = 1$$

where $M_p = 1,483,000$ in-lb and $S_p = 184,000$ lb. This leads to $P = 87,090.8$ lb. Figure B.3 shows the loading diagram and the corresponding shear and moment diagrams for the beam. Note that a hinge has not appeared at station 1. The following values are calculated as described earlier in this appendix with the exception that α is set equal to unity for conservative results: $U_s = 1612.1$ lb-in, $U_b = 10,676.8$ lb-in, and $U_t = 12,288.9$ lb-in. The load carrying capacity is now calculated using Eq. (18).

$$2w = \frac{4g(2-\beta)^2 U_t}{(1+\beta^2)\ V_0^2} - 125$$

$$= \frac{4(386.4)\ (1.5)^2\ (12,288.9)}{1.25\ (96)^2} - 125$$

$$= 3584.7 \text{ lb.}$$

Appendix C
THREE HINGED PROPPED BEAM

The presence of three plastic hinges occurring simultaneously in the propped beam is now examined. Consider the case for maximum motion occurring at the clamped end of the propped cantilever beam. The maximum loads acting on the beam are shown in Fig. C-1. Limit analysis indicates that for $\beta > 0.5$ there are plastic hinges at stations 1 and 3. However, since the interaction equation must be satisfied at the final location of the hinges, it can be shown that for

$$0.5 \leqslant \beta < 0.6265 \tag{C.1}$$

hinges occur at stations 2 and 3, while for

$$0.6265 < \beta \leqslant 1 \tag{C.2}$$

hinges occur at stations 1 and 3. When $\beta = 0.6265$ three hinges exist simultaneously at stations 1,2, and 3. This special case is now examined.

Assume that these three hinges exist simultaneously for the free body diagram of the beam in Fig. C-1. Consider the section of the beam just to the left of station 1 as shown in Fig. C-2 and the section of the beam just to the right of station 2 as shown in Fig. C-3. From Fig. C-2, $M = 30\ R_L$ and $S = R_L$. Substituting into Eq. (19) gives $R_L = 47,740$ lb as reported earlier.

For the hinges at stations 2 and 3 consider Fig. C-3 where $R_R = S$ and $M = M_R$ since Eq. (19) is satisfied simultaneously at these stations. Thus, $30\ R_R = 2\ M_R$ or $M_R = 15\ R_R$. Now

$$\left(\frac{R_R}{S_p}\right)^2 + \left(\frac{15\ R_R}{M_p}\right)^2 = 1$$

so that $R_R = 87,091$ lb and $M = 1,306,361$ in.-lb. Applying these reactions to Fig. C-1, the allowable loads are found such that $\beta = 0.6265$ and $P = 82,896$ lb.

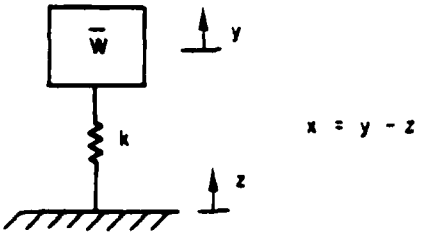

Fig. 1 — Single degree of freedom system

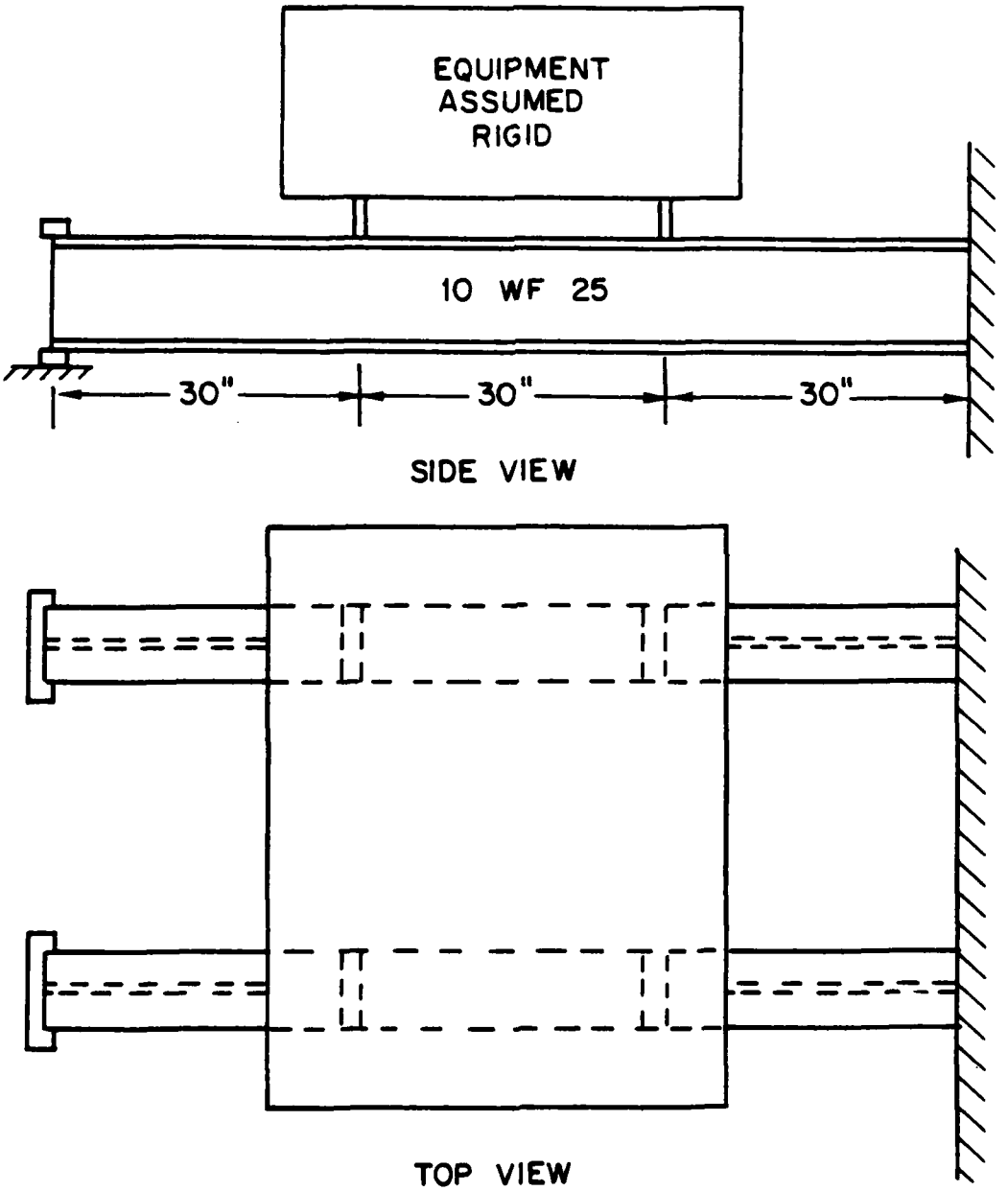

Fig. 2 — Equipment-foundation combination

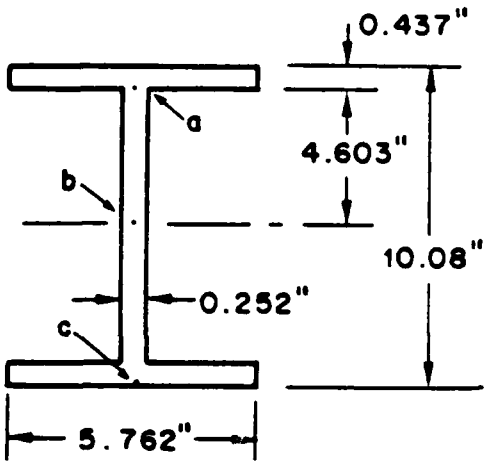

AREA = 7.35 in^2
WEB AREA = 2.32 in^2
FLANGE AREA = 2.52 in^2
I_{xx} = 133.2 in^4

Fig. 3 — 10 WF 25 beam properties

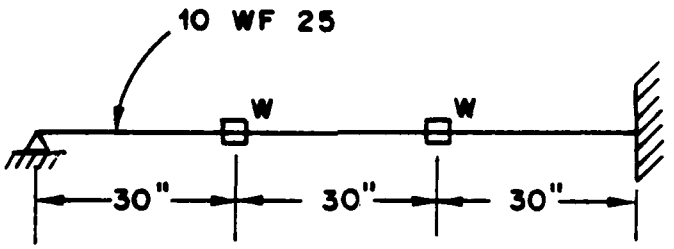

Fig. 4 — Model of equipment-foundation combination

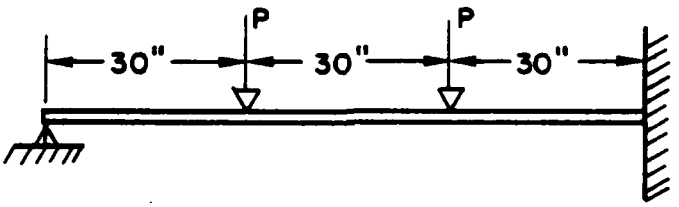

Fig. 5 — Loads acting on beam foundation

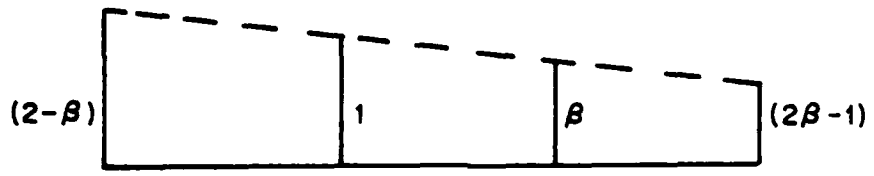

(a) Maximum motion at the pinned end

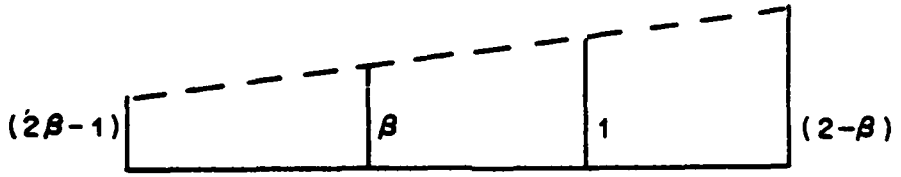

(b) Maximum motion at the clamped end

Fig. 6 — Shock excitation models for unequal foundation support motion

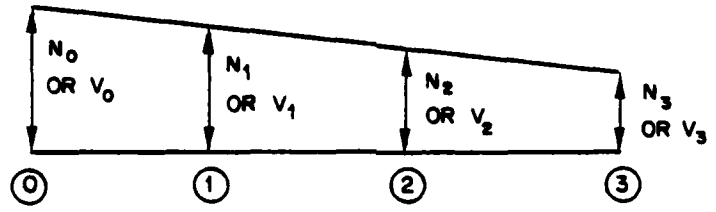

(a) Maximum motion at the pinned end

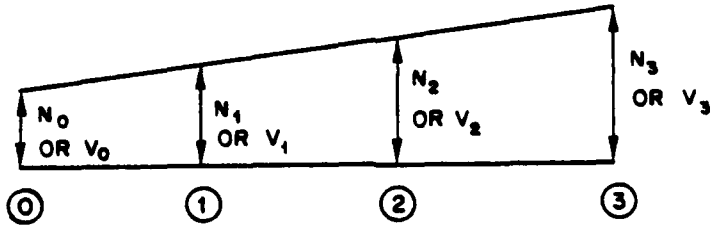

(b) Maximum motion at the clamped end

Fig. 7 — Shock excitation levels for unequal foundation support motion

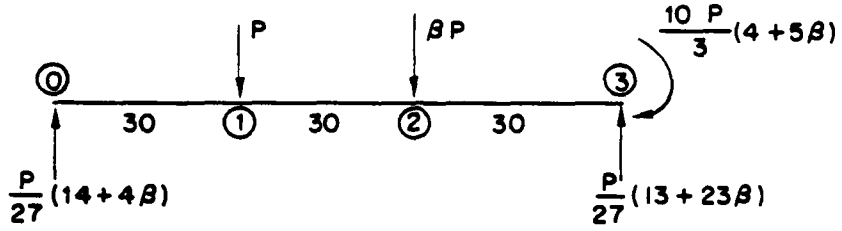

(a) Free-body diagram

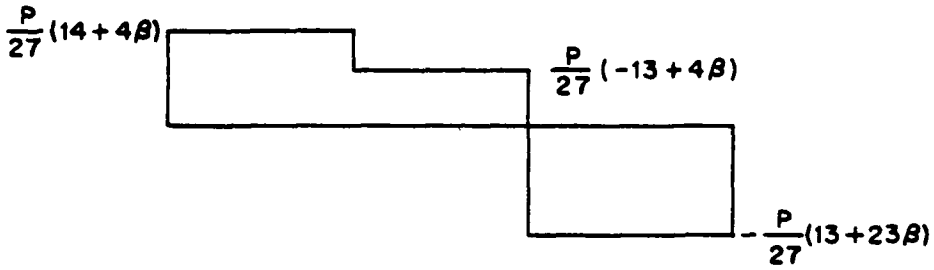

(b) Shear diagram

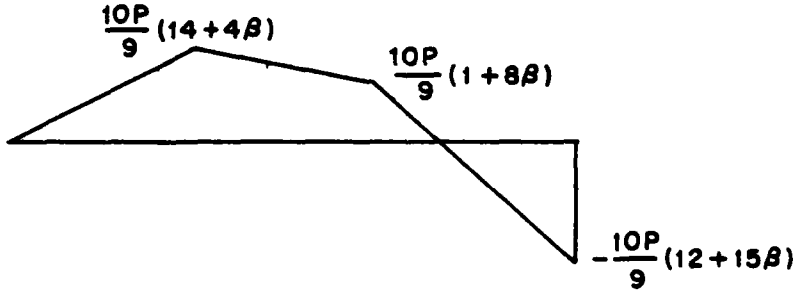

(c) Moment diagram

Fig. 8 — Elastic analysis of the propped beam for maximum shock motion of the pinned end

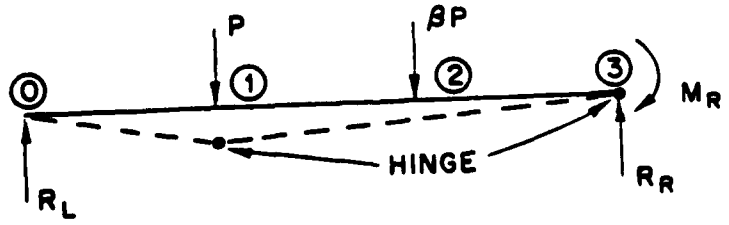

Fig. 9 — Plastic hinges for maximum shock motion of the pinned end

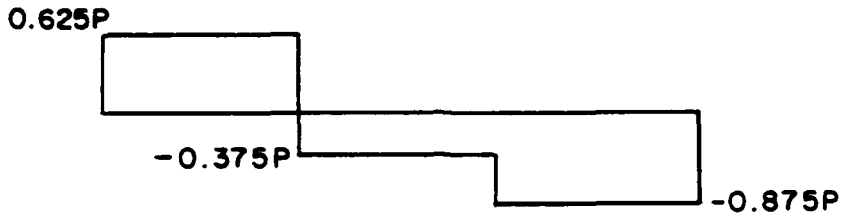

(a) Shear diagram

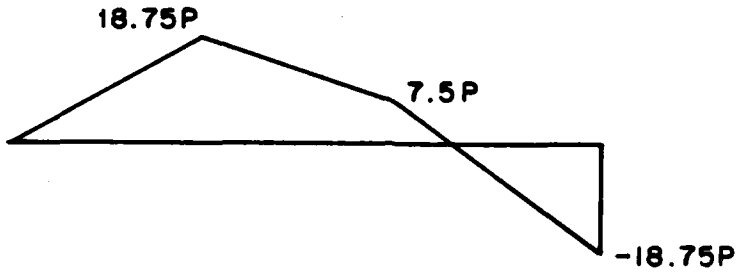

(b) Moment diagram

Fig. 10 — Shear and moment diagrams by limit analysis for maximum shock motion of the pinned end, $\beta = 0.5$, and $P = 75,750$ lb

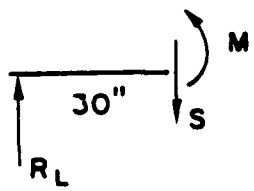

Fig. 11 — Free body diagram of the beam to the left of station 1

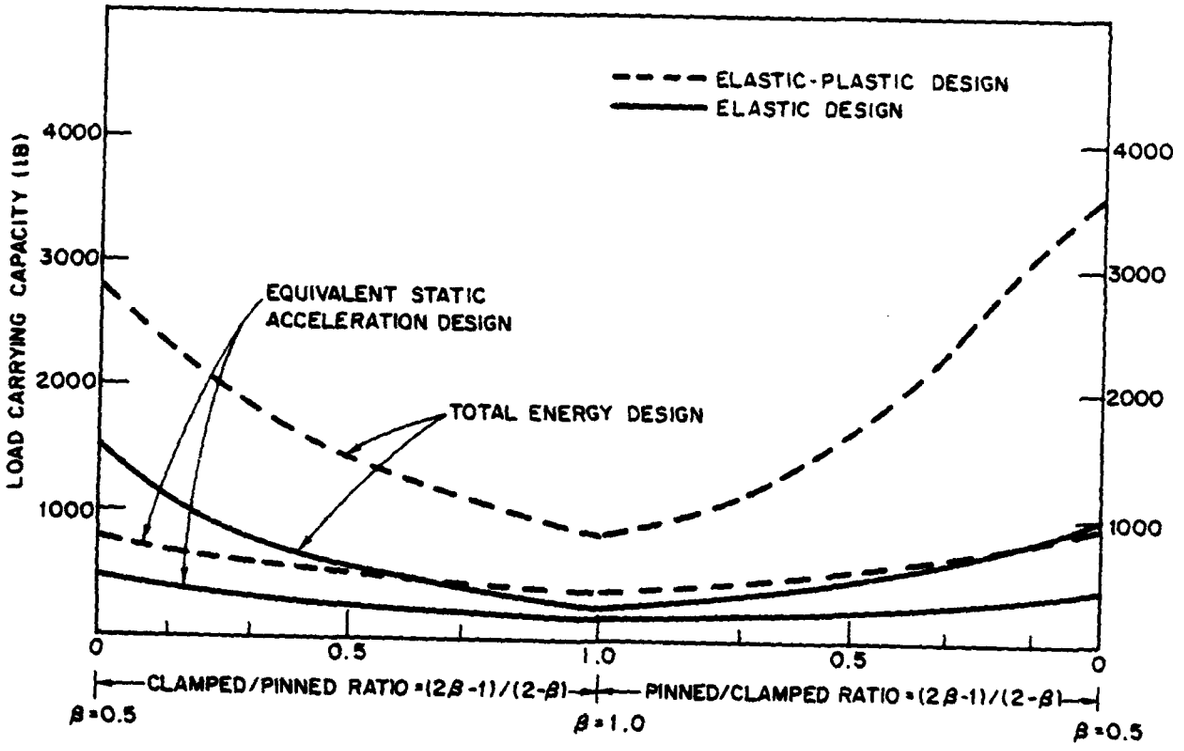

Fig. 12 — Load carrying capacity of one propped beam

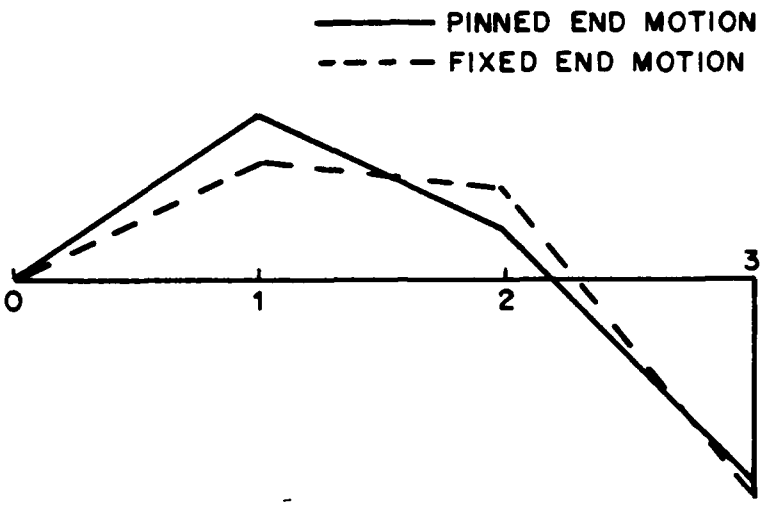

(a) Elastic design

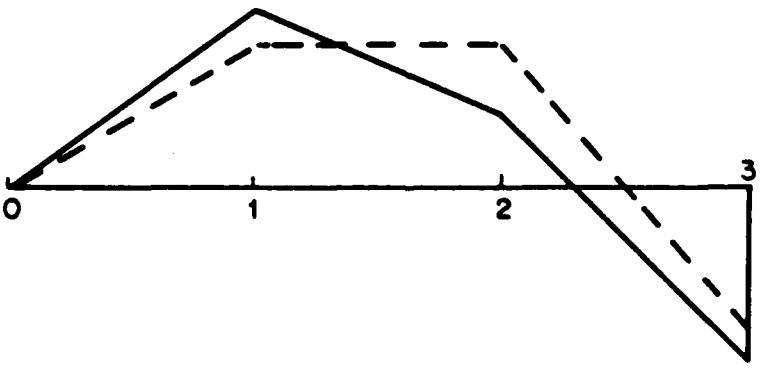

(b) Elastic-Plastic design

Fig. 13 — Bending moment diagrams for $\beta = 0.5$

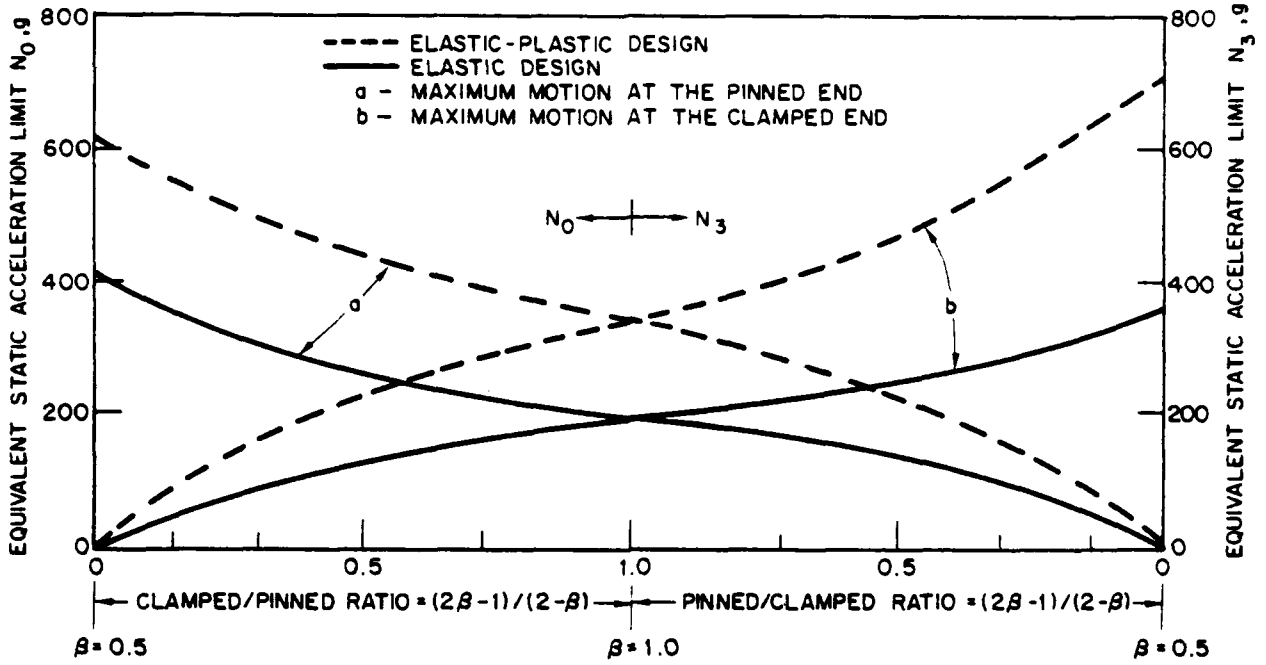

Fig. 14 — G-load limits for elastically designed structure, $2w$ = 242.0 lb

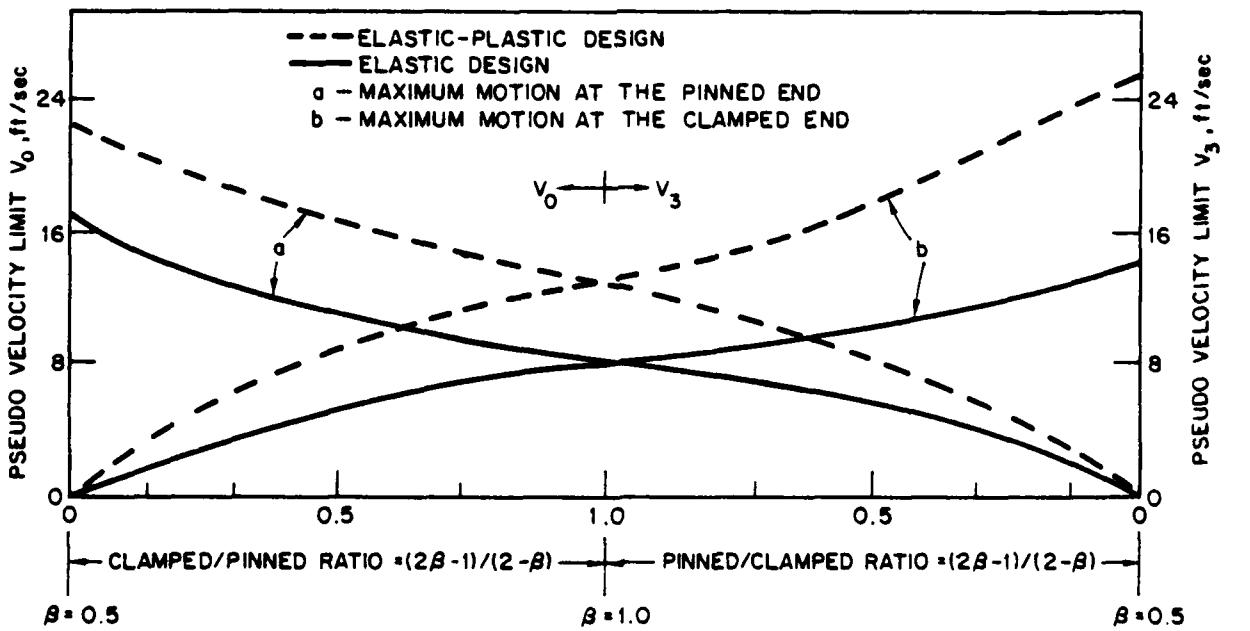

Fig. 15 — Design shock spectrum velocity limits for elastically designed structure, $2w$ = 242.0 lb

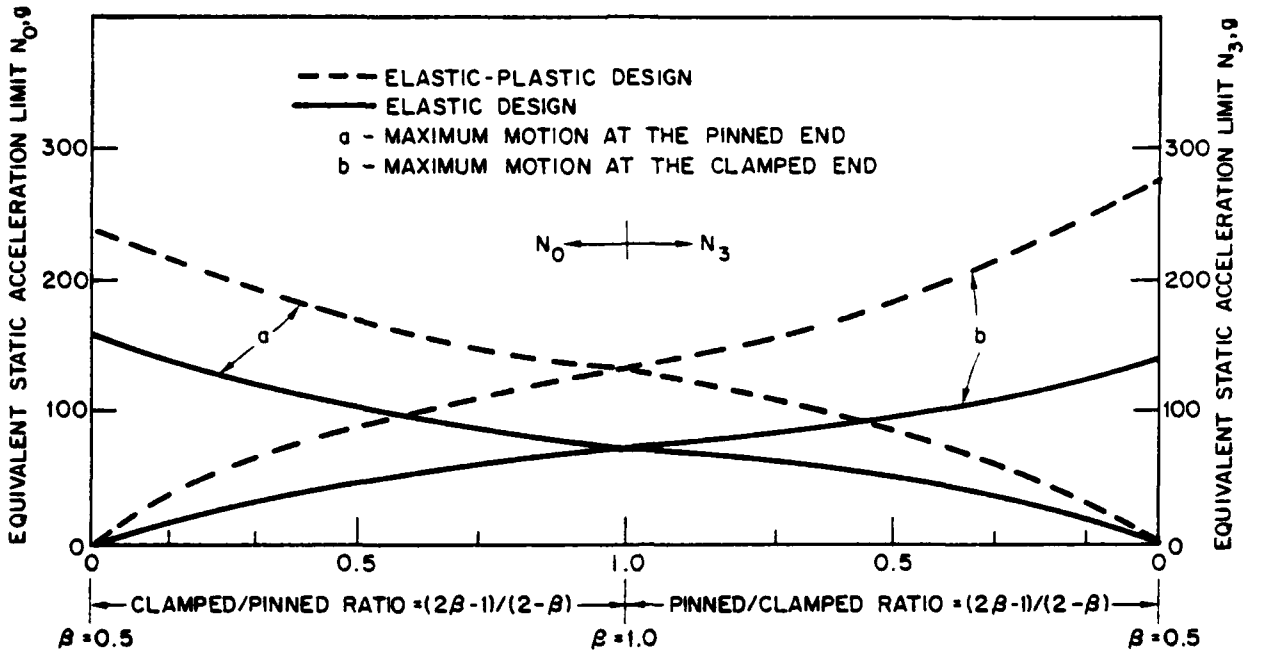

Fig. 16 — G-load limits for elastic-plastically designed structure, $2w$ = 828.8 lb

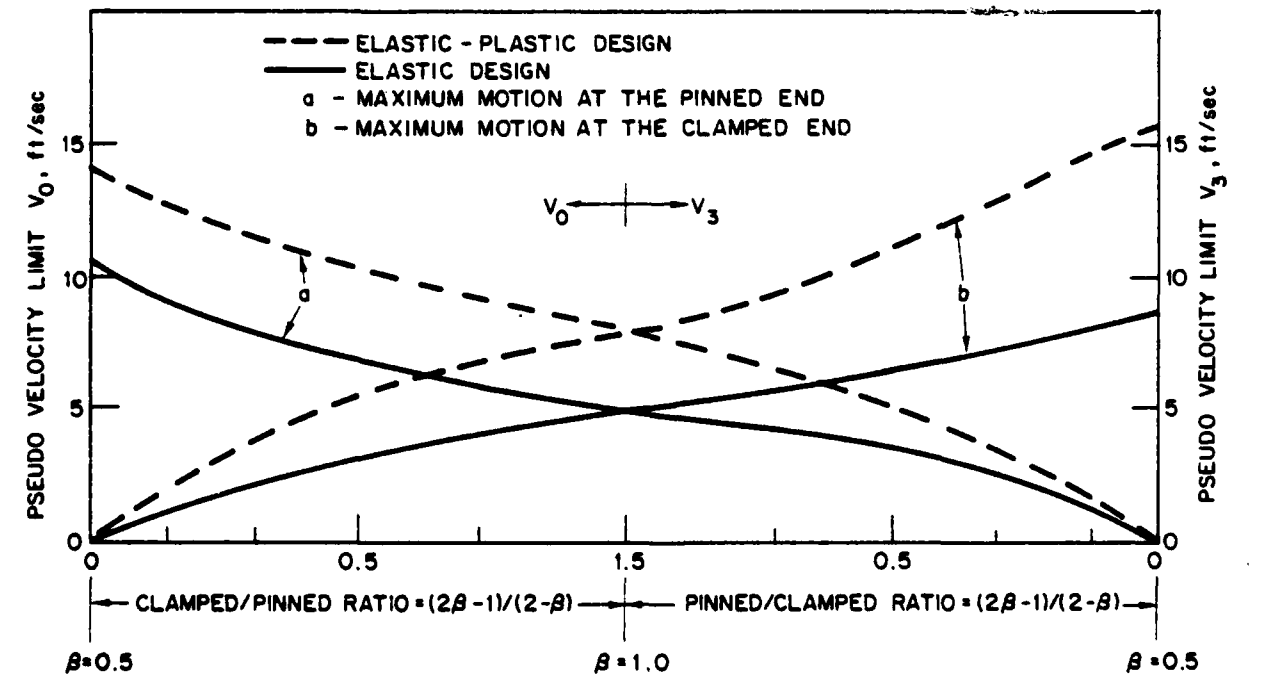

Fig. 17 — Design shock spectrum velocity limits for elastic-plastically designed structure, $2w$ = 828.8 lb

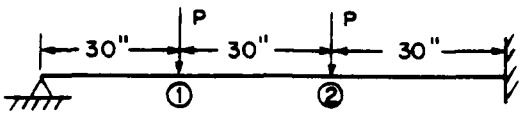

Fig. A-1 — Propped cantilever beam

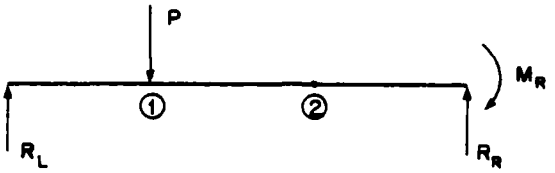

Fig. A-2 — Free body diagram with load acting at station 1

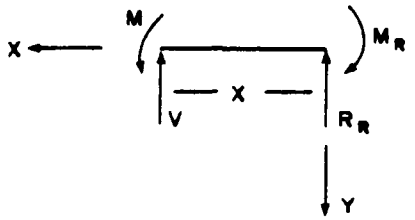

Fig. A-3 — Coordinate system for computing deflections

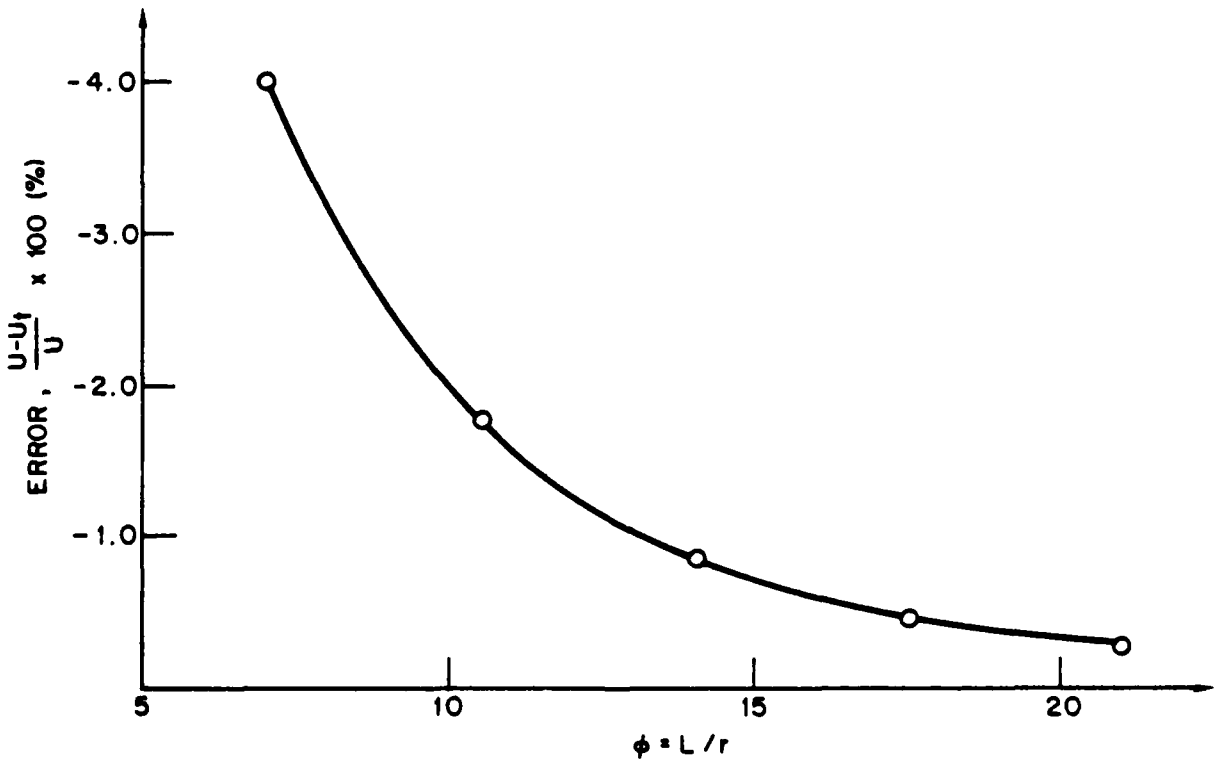

Fig. A-4 — Percent error in energy calculations when shear effects in beam reactions and deflections are ignored

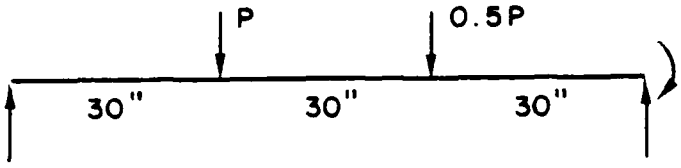

(a) Loading diagram

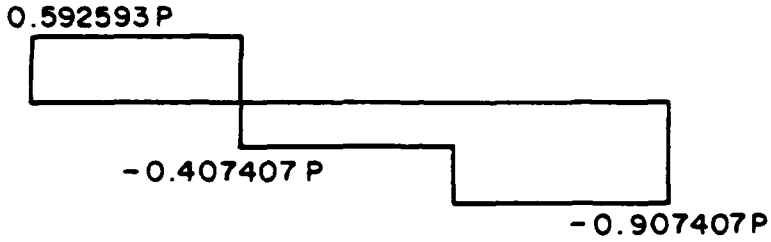

(b) Shear diagram

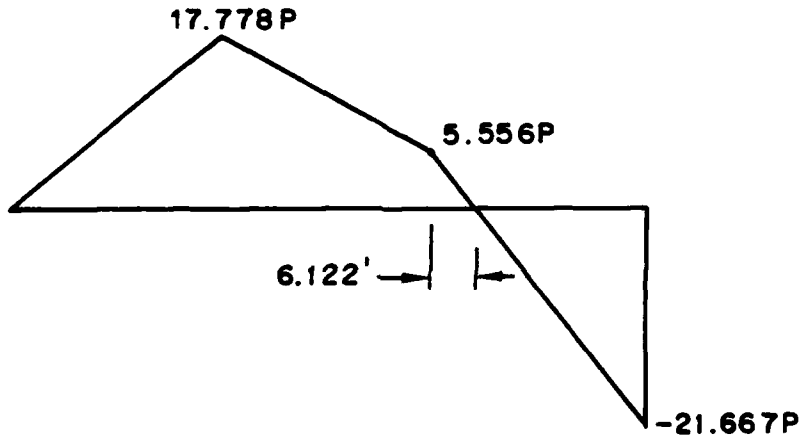

(c) Moment diagram

Fig. B-1 — Elastic analysis of the propped beam, $\beta = 0.5$

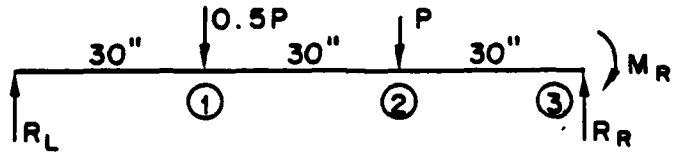

(a) Free body diagram

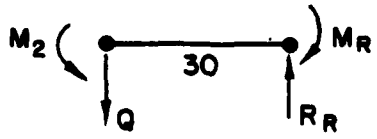

(b) Section to the right of station 2

Fig. B-2 — Maximum motion at the clamped support, $\beta = 0.5$

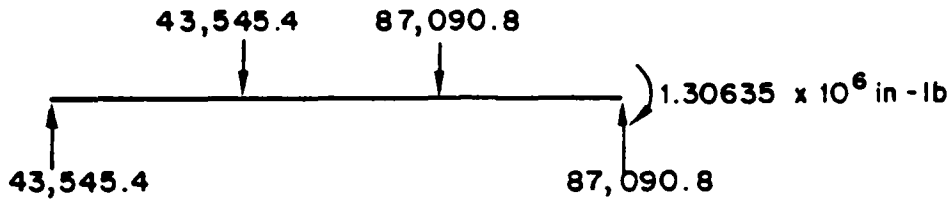

(a) Loading diagram

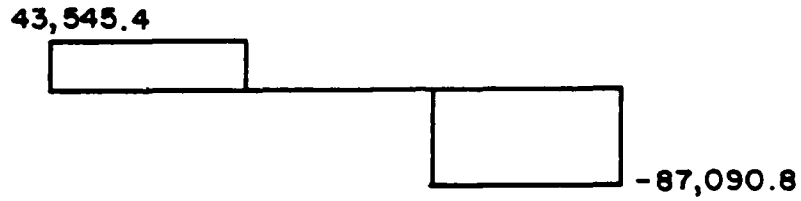

(b) Shear diagram

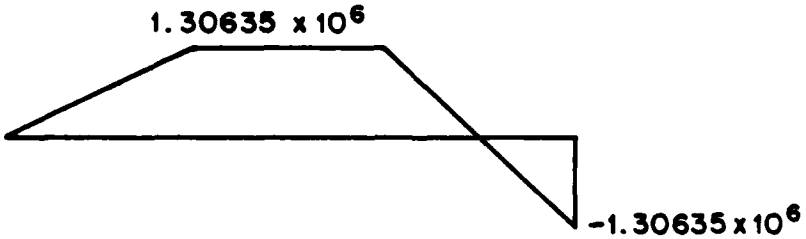

(c) Moment diagram

Fig. B-3 — Elastic-plastic analysis for maximum motion at the clamped support, $\beta = 0.5$

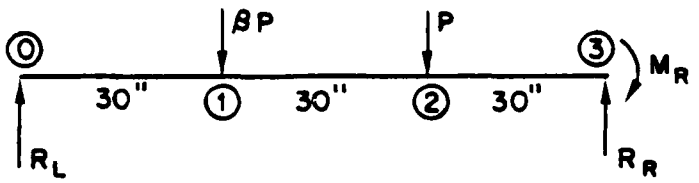

Fig. C-1 — Free body diagram for maximum motion at the clamped end

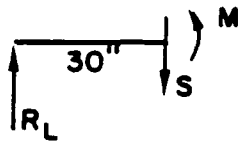

Fig. C-2 — Section to the left of station 1

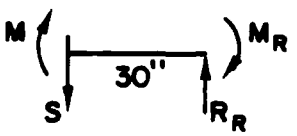

Fig. C-3 — Section to the right of station 2